Chapter 4
On-Panel Analog Output Buffer for Data Driver with Consideration of Device Characteristic Variation

4.1 INTRODUCTION

Based on chapter 1, we know that the LTPS TFTs have been widely investigated as a material for portable systems, such as digital camera, mobile phone, personal digital assistants (PDAs), notebook, and so on, because the electron mobility of LTPS TFTs is about 100 times larger than that of the conventional amorphous silicon TFTs. Furthermore, LTPS can achieve slim, compact, and high-resolution display by integrating the driving circuits on peripheral area of display. If the mobility of poly-Si TFTs is further increased, this technology will become more suitable for realization of SoP applications that will integrate with memory, CPU, and display [18], [19].

At present, LTPS technology has a tendency towards integrating all control circuits and driver circuits on the glass substrate [20], [21]. In general, the LCD driver contains gate driver, data driver, and DC-DC converter. The data driver is composed of shifter registers, latch, level shifters, D/A converters, and analog output buffer. The last two components belong to the analog circuit region. A novel 6-bit DAC has been proposed in last chapter. However, the analog output buffer is also a critical design to achieve the low power dissipation, high resolution, and large output swing on LCD panel. For this reason, an on-panel analog output buffer for data driver with consideration of device characteristic variation will be proposed in this chapter.

4.2 DEVICE CHARACTERISTIC VARIATION IN LTPS TECHNOLOGY

Although using LTPS process can enlarge poly-grain size to improve the device performance, it usually accompanies a random device-to-device variation on LCD panel. The harmful effects of irregular grain boundaries, gate-insulator interface defects, and incomplete ion-doping activation in thin poly-silicon channels result in the variation on electrical characteristics of LTPS TFTs. Fig. 4.1 shows the variation on threshold voltage (V_{TH}) of 120 LTPS n-type TFTs in different locations on LCD panel. The V_{TH} of LTPS n-type TFTs in different panel locations has wide distribution from 0.75 V to 2.15 V [22]. The device characteristic variations of LTPS p-type TFTs in different gate bias are shown in Fig. 4.2 [23]. Based on these two figures, the device characteristic variations in LTPS technology are quite large compared with CMOS technology.

However, in spite of many advantages of LTPS technology, main applications are still limited to small size displays. The reason is that the poly-Si TFTs have poor uniformity and suffer from large variations on the device characteristics due to the narrow laser process window for producing large-grained poly-Si thin film. The random grain boundaries and trap density exist in the channel region. This leads to some problems in real product applications such as non-uniformity brightness in panel, error reading in digital circuits, current gain mismatching in analog circuits, and so on [24]. As a result, the device characteristic variation becomes a very serious problem for analog circuit design in LTPS technology [25].

In this work, a class-A analog output buffer with suppressing device variation method has been proposed. By this proposed method, the manufacturing yield of the circuit can be increased and the performance of the on-panel analog output buffer also can be maintained effectively.

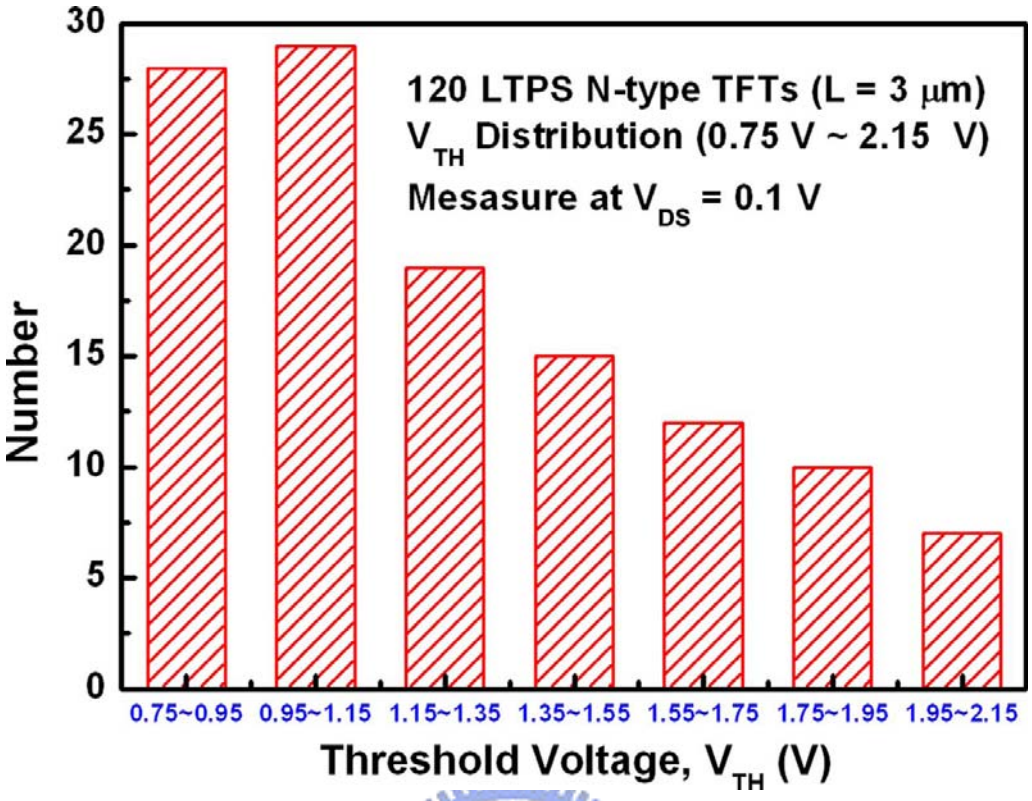

Fig. 4.1 Variation on threshold voltage (V_{TH}) of 120 LTPS n-type TFTs in different locations on LCD panel.

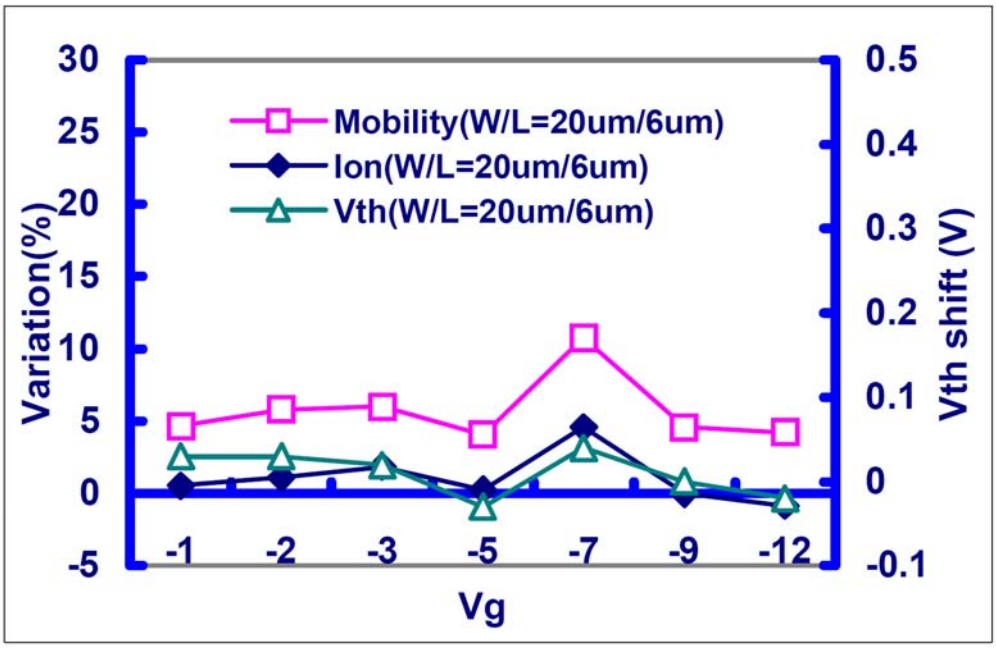

Fig. 4.2 The device characteristic variations of LTPS p-type TFTs in different gate bias.

4.3 ON-PANEL ANALOG OUTPUT BUFFER

4.3.1 Source Follower Analog Output Buffer [26]

The conventional source follower output buffer has been integrated on the glass substrate for data driver. However, there are some drawbacks in such output buffer including the lower output swing and the higher input offset voltage. Fig. 4.3 shows the circuit of the conventional source follower output buffer and its output waveforms at different input voltages. From this figure, we can find that the output swing of the source follower output buffer is limited to V_{DD}–V_{th}. Besides, there is always an input offset voltage in the source follower output buffer due to the threshold voltage of the TFT. The output swing and input offset voltage of source follower output buffer are not constant values, because these are both related to the various threshold voltages of the TFTs in different panel locations. The Monte Carlo simulation results of source follower output buffer is shown in Fig. 4.4.

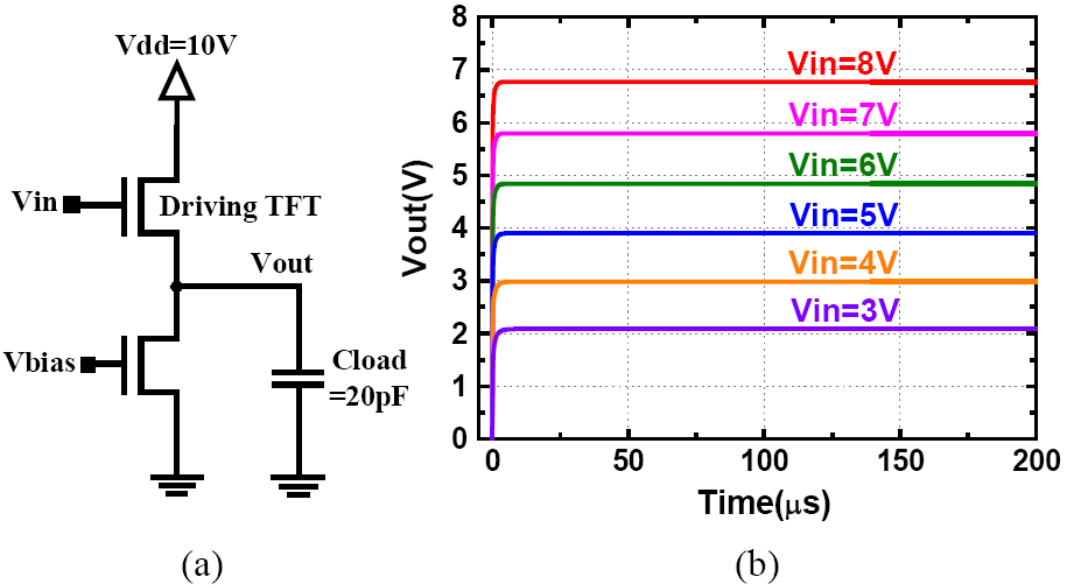

Fig. 4.3 (a) The conventional source follower output buffer and (b) its output waveforms at different input voltages.

Although the source follower output buffer has a huge input offset voltage, the input offset voltage can be reduced by using some compensation technique, like Fig. 4.5 shown. The additional switch devices, capacitors, and control signals are necessary for these methods. The power consumption of this output buffer will become an important issue due to the extra V_{bias} voltage and the DC current path.

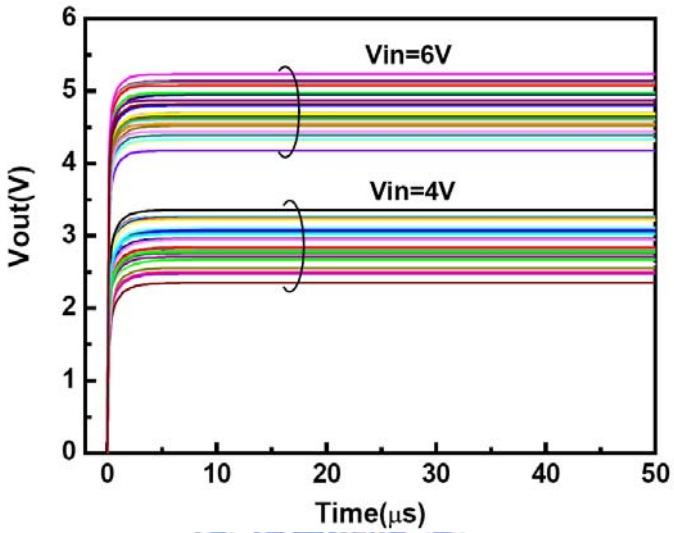

Fig. 4.4 The Monte Carlo simulation results of the conventional source follower output buffer.

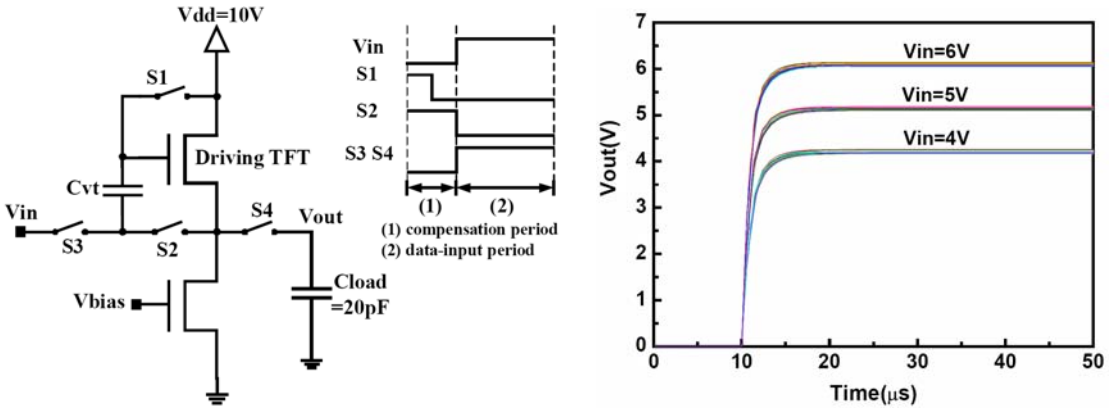

(a) (b)

Fig. 4.5 (a) The source follower output buffer with V_{TH} compensation method and (b) Monte Carlo simulation results of this source follower output buffer.

4.3.2 Unity-Gain Output Buffer with an OPAmp

The conventional source follower output buffer has lower output swing and larger input offset voltage. In opposition to the source follower output buffer, the unity-gain output buffer with an OP amp has lower input offset voltage. The relation function between the input and output of this output buffer is

$$V_o = \frac{A}{1+A} V_{in} \qquad (4 - 1)$$

For this reason, the input offset voltage can be reduced by the large open-loop gain (A) of the unity-gain output buffer with an OP amp. In this work, the two-stage OP amp is adopted as a unit-gain output buffer, since the two-stage OP amp has higher open-loop gain, as well as the OP amp has high immunity to noise. Furthermore, the unity-gain output buffer with an OP amp has a larger slew rate for driving the capacitance load of the data bus on panel than that of source follower output buffer at the same operation frequency.

The circuit diagram of the class-A analog output buffer with N-TFTs input stage is shown in Fig. 4.6. As a unity-gain buffer, the output node (Vo) is connected to the negative input node (Vi-) and the input signal is applied to the positive input node (Vi+). This output buffer comprises four parts as following. The first part consists of an n-channel differential pair (M1-M2) with a p-channel current mirror load (M3-M4) and an n-channel tail current source (M5). The second part is a common-source amplifier stage (M6-M7), which can improve the open-loop gain and reduce the input offset voltage for this output buffer. The bias generator part is a constant g_m bias circuit (M11-M16 and R_B), which can provide the bias voltages for this output buffer. By using constant g_m bias method, a more steady reference voltage can be generated due to the constant g_m value.

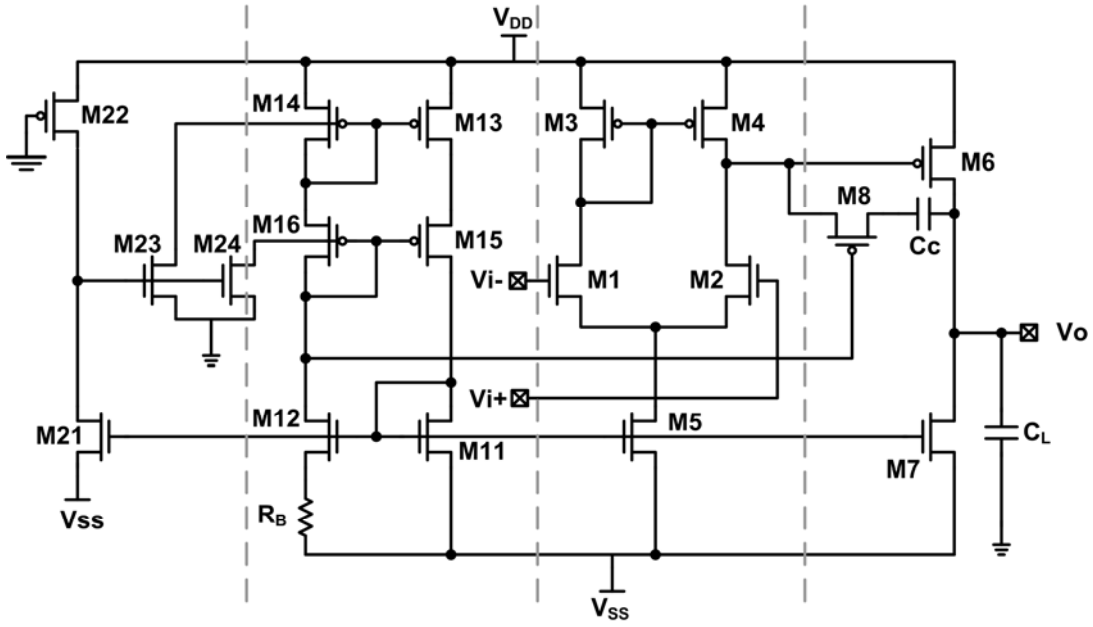

Fig. 4.6 The class-A analog output buffer with N-TFTs input stage.

However, the bias circuit is a self-biasing circuit, it needs a start-up circuit (M21-M24) that turns on the bias circuit in the beginning and automatically be turned off after bias circuit working.

Since there are two poles in this unity-gain output buffer circuit, the OP amp circuit needs frequency compensation to improve the phase margin and stability of the OP amp. In this work, the Miller compensation technique with nulling resistor (M8 and C_C) is adopted as frequency compensation circuit, which can provide a negative zero as

$$z = \frac{1}{(1/g_{m6} - R_C)C_C} \qquad (4 - 2)$$

where the resistor R_C is implemented by using a P-type TFT (M8) biased in the triode region. Making the resistance (R_C) greater than $1/g_{m6}$ moves the zero into the left half-plane (LHP), which can be used to provide positive phase shift at high frequency region and consequently to improve the phase margin of this output buffer.

The simulated frequency response and circuit performances of this output buffer are shown in Fig. 4.7 and Table 4.1, respectively.

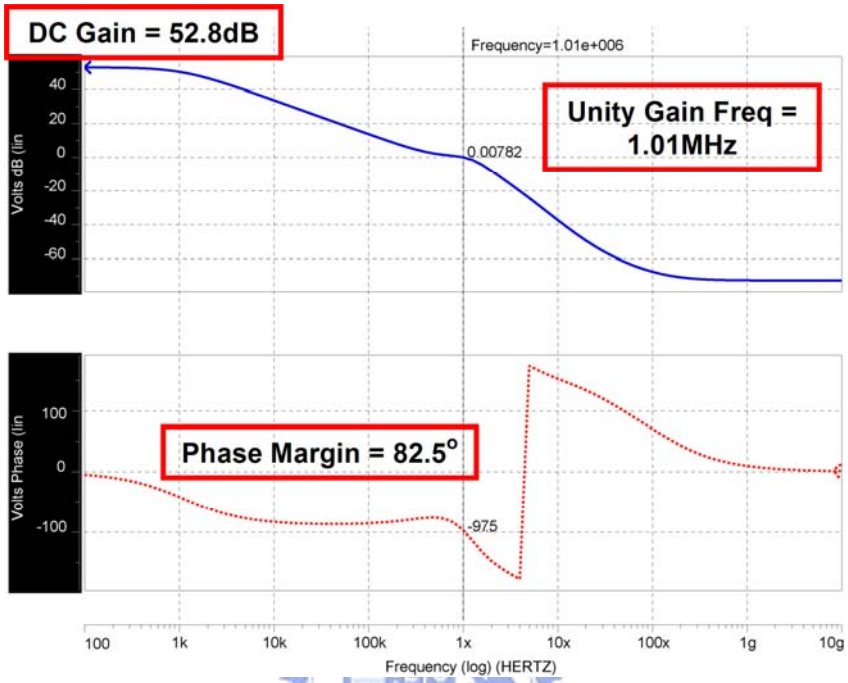

Fig. 4.7 The simulated frequency response of the class-A analog output buffer with N-TFTs input stage in open-loop condition.

Table 4.1

Summary of the simulated circuit performances of the output buffer in Fig. 4.6.

Open-Loop Characteristics	
Differential Gain	52.8 dB
Phase Margin	82.5 °
Unity Gain Bandwidth	1.01 MHz
CMRR	57.81 dB
PSRR + (–)	58.7 (62.2) dB
Close-Loop Characteristics	
Output Swing	1.8 ~ 9.2 V
Slew Rate	1.510 V/μs
Average Power Dissipation	1.386 mW
Power Supply	V_{DD} = 10 V, V_{SS} = 0 V

4.3.3 Proposed Output Buffer with Suppressing Device Variation

Based on section 4.2, we can find that the threshold voltages of the N-type TFT devices in different panel locations vary from 0.75 V to 2.15 V, whose variation is quite large compared with CMOS technology [22]. Besides, the device characteristic variation of the N-type TFT is more serious than that of P-type TFT [27]. For example, the mobility variation of N-type TFT and P-type TFT under the hot-carrier stress are -38.627% and +7.054%, respectively [28]. The average of mobility variation for n-channel and p-channel TFTs at different stress conditions are shown in Table 4.2.

For this reason, replacing the critical part of the analog circuit by P-TFTs is a valid technique for suppressing device characteristic variation and improving the manufacturing yield of the analog circuit. In this unity-gain output buffer, the differential pair of the OP amp is the critical part. Therefore, the output buffer with P-TFTs input differential pair is proposed to suppress the device variation in this work. This proposed output buffer with P-TFTs input stage can be operated at 50-kHz operation frequency with an output voltage swing of 1-to-9 V

Table 4.2
Mobility variation for n-channel and p-channel TFTs at different stress conditions.

		Average Variation (%)	**Std. Dev**
Hot-Carrier Stress Condition	***N-Channel***	-38.627	6.65
	P-Channel	+7.054	2.72
On-Current Stress Condition	***N-Channel***	+11.828	3.28
	P-Channel	+2.251	0.6525

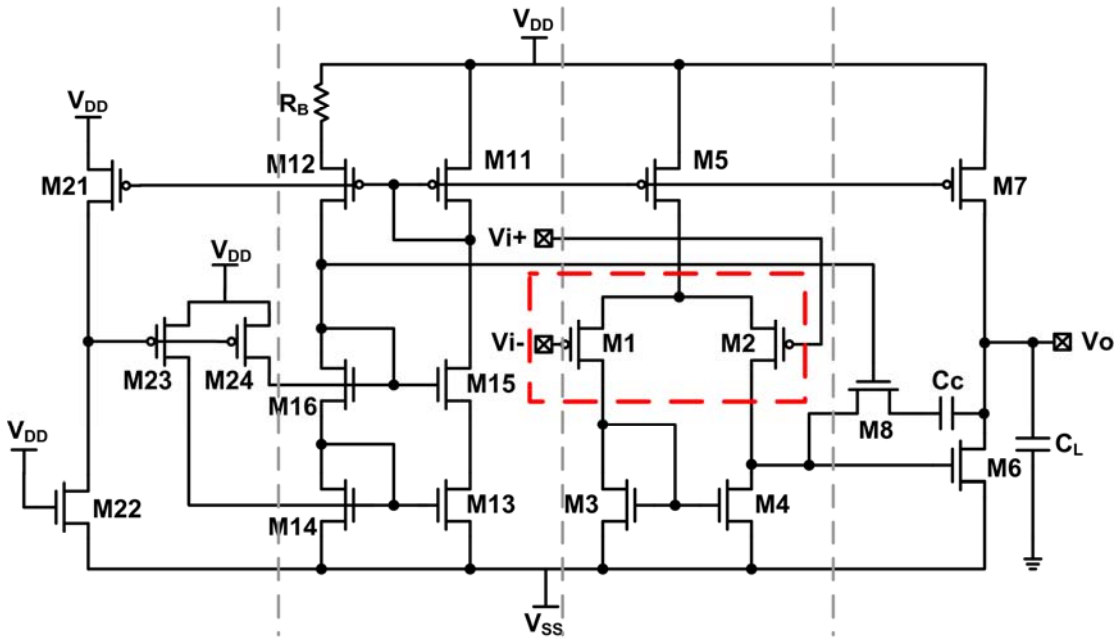

Fig. 4.8 The class-A analog output buffer with P-TFTs input stage.

The proposed analog output buffer with P-TFTs input stage is shown in Fig. 4.8. These two OP amps (in Fig. 4.6 and Fig. 4.8) have the similar dc voltage gain, as shown in the following

$$A_V(0)_{N-input} = g_{m1-N} \cdot g_{m6-P} \cdot R_1 \cdot R_2 \qquad (4-3)$$

$$A_V(0)_{P-input} = g_{m1-P} \cdot g_{m6-N} \cdot R_1 \cdot R_2 \qquad (4-4)$$

where R_1 is the value of r_{o2} parallel with r_{o4} and R_2 is the value of r_{o6} parallel with r_{o7}. From equations (4 - 3) and (4 - 4), the dc voltage gain of OP amp with P-TFTs input stage is almost similar to that of OP amp with N-TFTs input stage, when $(W/L)_1$ and $(W/L)_6$ are designed with the same device dimensions.

There are some advantages in the OP amp with P-TFTs input stage compared with the OP amp with N-TFTs input stage. The OP amp with P-TFTs input stage has larger unity-gain frequency since $\omega_u \sim |p_2| = g_{m6}/C_L$ and g_{m6-N} is larger than g_{m6-P}.

Furthermore, this OP amp with P-TFTs input stage also has better slew rate than the OP amp with N-TFTs input stage due to the larger unity-gain frequency in the OP amp with P-TFTs input stage. The OP amp with P-TFTs input stage also has more steady circuit performances, because the critical part (differential pair) of the OP amp is composed of the P-TFTs which have less device characteristic variation. The simulated frequency response and comparison on circuit performances are shown in Fig. 4.9 and Table 4.3, respectively. From this simulation results, we can find that the circuit performances in this proposed output buffer also can be maintained nearly the same as the performances in the output buffer with N-TFTs input stage

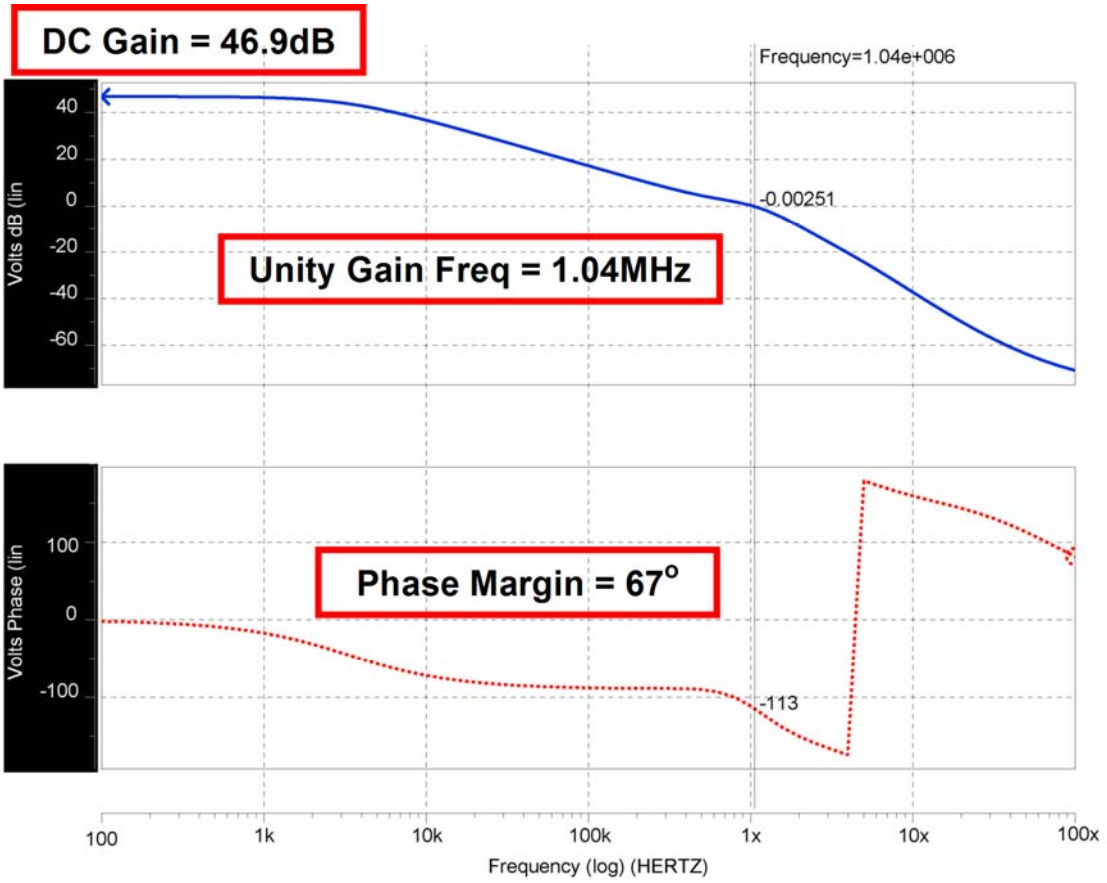

Fig. 4.9 The simulated frequency response of the class-A analog output buffer with P-TFTs input stage in open-loop condition.

Table 4.3
The summary and comparison of the simulated circuit performances of the output buffer in Fig. 4.6 and Fig. 4.8.

Open-Loop Characteristics		
Output Buffer Type	***N-TFTs input stage OP amp***	***P-TFTs input stage OP amp***
Differential Gain	52.8 dB	46.9 dB
Phase Margin	82.5 °	67 °
Unity Gain Bandwidth	1.01 MHz	1.04 MHz
CMRR	57.81 dB	59.3 dB
PSRR + (–)	58.7 (62.2) dB	76.3 (52.3) dB
Close-Loop Characteristics		
Output Swing	1.8 ~ 9.2 V	0.91 ~ 9.1 V
Slew Rate	1.510 V/μs	1.885 V/μs
Average Power Dissipation	1.386 mW	1.734 mW
Power Supply	V_{DD} = 10 V, V_{SS} = 0 V	V_{DD} = 10 V, V_{SS} = 0 V

Besides, the P-TFTs have less flicker noise (1/f noise) than that of N-TFTs, since holes are less likely to be trapped. For this reason, the proposed output buffer with P-TFTs input stage has better flicker noise (1/f noise) performance than that of the output buffer with N-TFTs input stage. Moreover, the proposed output buffer with P-TFTs input stage also has other advantages, such as larger slew rate, lower input offset voltage, and better immunity to noise, as comparing to the source follower output buffer. The proposed output buffer with P-TFTs input stage can be operated at 50-kHz operation frequency with an output voltage swing of 1-to-9 V. The power supply of this circuit is V_{DD} of 10 V and V_{SS} of 0 V.

4.4 EXPERIMENTAL RESULTS

The class-A output buffers with N-TFTs input stage and P-TFTs input stage have been design and fabricated in a 8μm LTPS technology. The photographs of these buffers on glass substrate with the corresponding pin names are shown in Fig. 4.10 (a) and Fig. 4.10 (b), respectively.

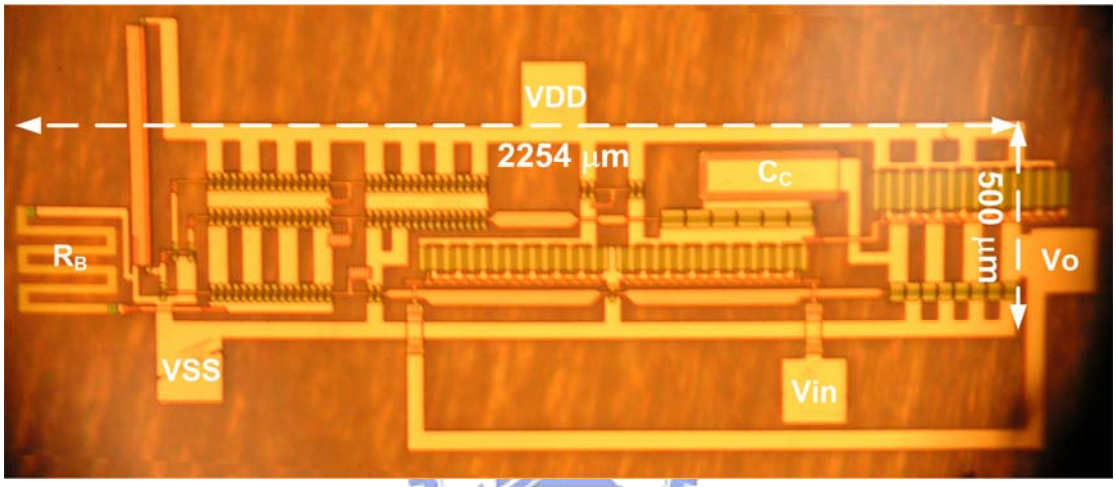

(a)

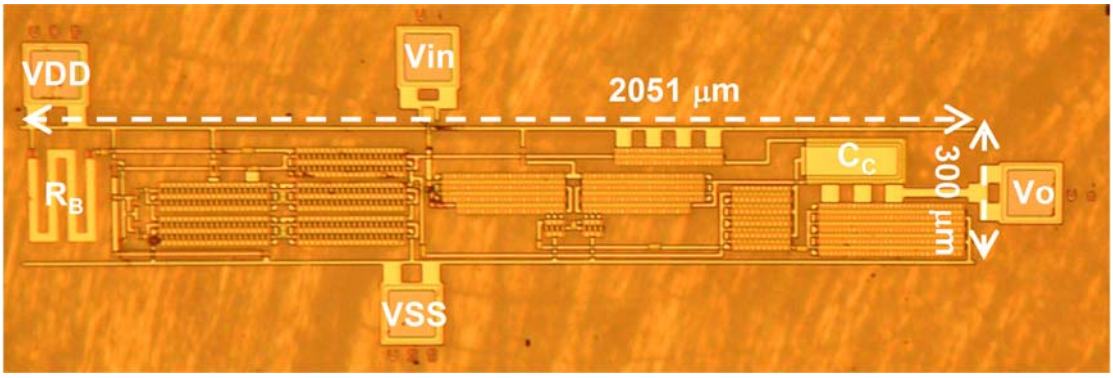

(b)

Fig. 4.10 The photographs of the class-A output buffers with (a) N-TFTs input stage and (b) P-TFTs input stage.

The setup illustrations for slew rate, output swing, and unity-gain bandwidth measurement are shown in Fig. 4.11 and Fig. 4.12, respectively. Tektronix TDS 3054 is an oscilloscope using to detect and display the signal waveforms. HP 4156B is a semiconductor parameter which can provide a V_{DD} of 10 V and V_{SS} of 0 V. Agilent 81110A and HP 8116A are function generators which can provide input signals, like square waveform or sine waveform. These instruments are used to measure the fabricated output buffer circuit.

Fig. 4.13 shows the proposed analog output buffer under the PCB (printed circuit board) with wire bonding and the measurement setup illustration with the wire bonding glass substrate samples. The glass samples under the PCB with wire bonding has more flexible measurement method for other application and demonstration.

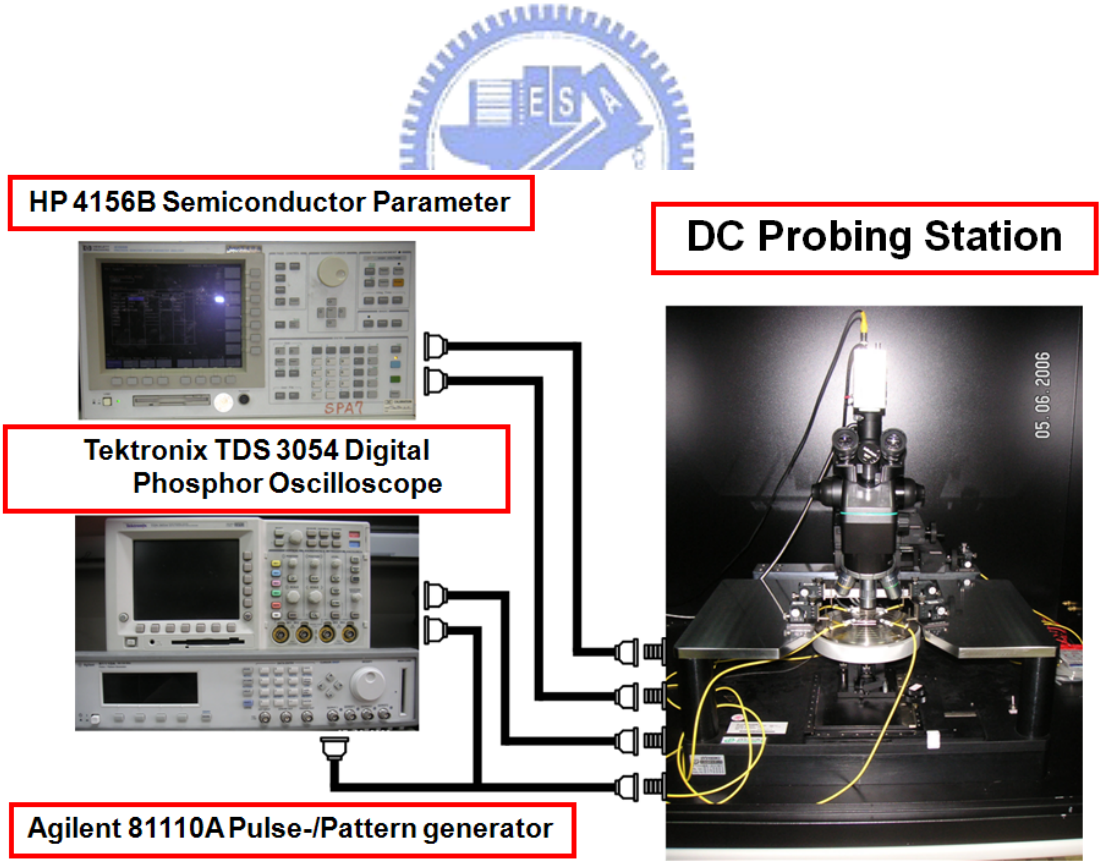

Fig. 4.11 The setup illustration for slew rate and output swing measurement with DC probing station.

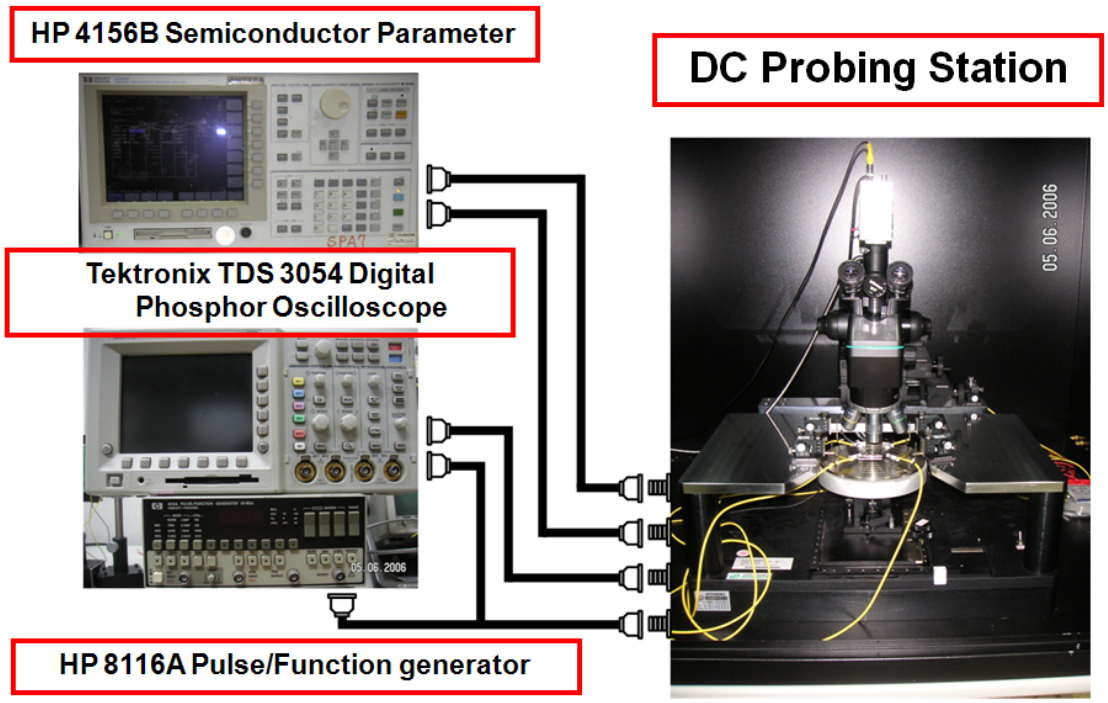

Fig. 4.12 The setup illustration for unity-gain bandwidth measurement with DC probing station.

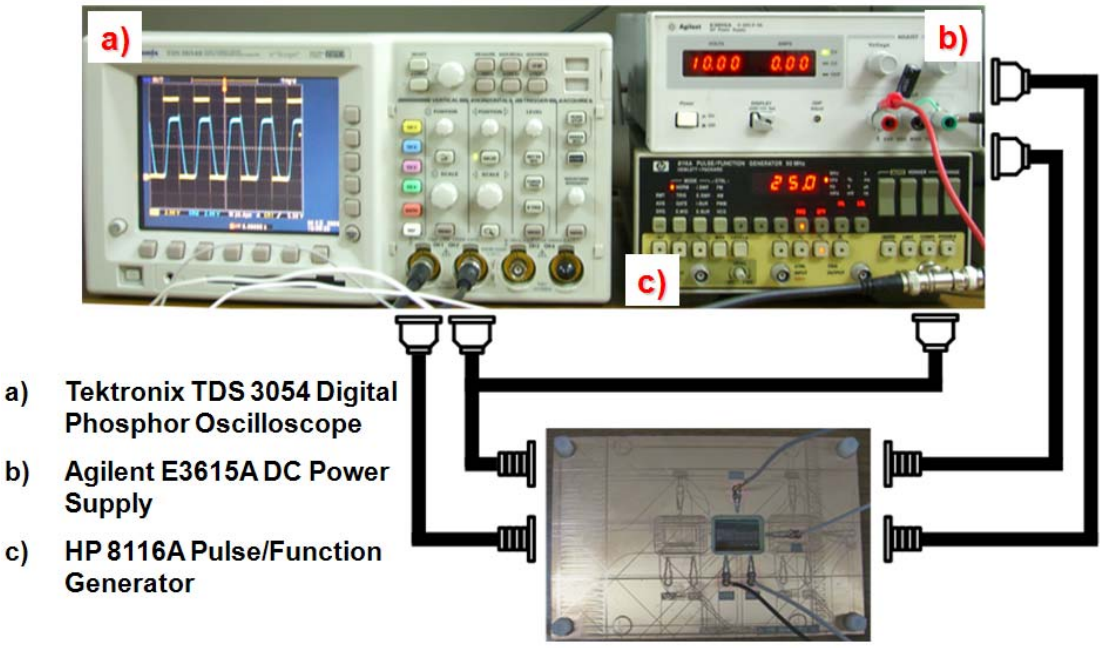

Fig. 4.13 The proposed analog output buffer under the PCB with wire bonding and the measurement setup illustration with the wire bonding glass substrate samples.

The measured output waveforms of class-A output buffers with N-TFTs input stage and P-TFTs input stage are compared in Fig. 4.14 and Fig. 4.15. Based on Fig. 4.14, we can find that the slew rate (output swing) of these two output buffers are 1.843 V/ms (0.2-to-6.8 V) and 1.961 V/ms (0.8-to-9.6 V), respectively. Moreover, from Fig. 4.15, the unity-gain bandwidth of these two output buffers are 55.6 kHz and 107.2 kHz, respectively.

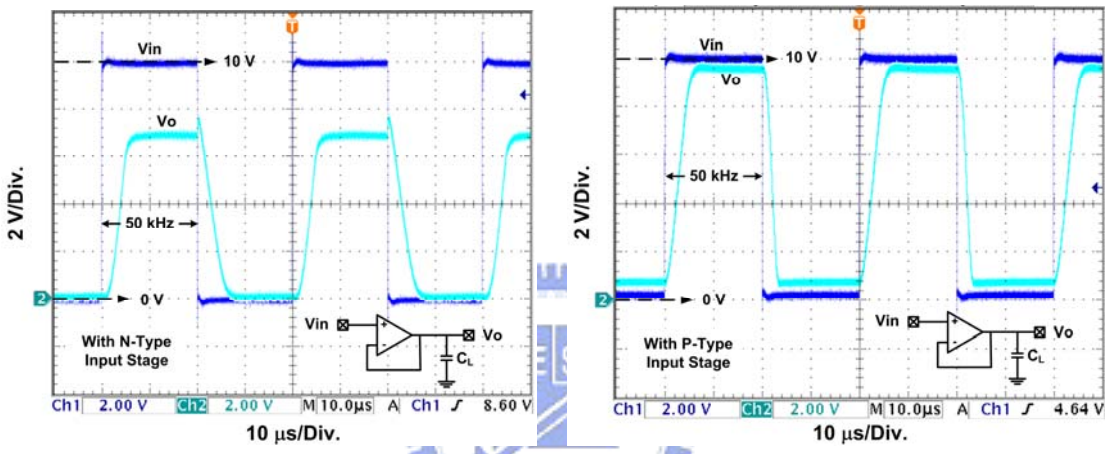

Fig. 4.14 The measured output waveforms of the class-A output buffers with (a) N-TFTs input stage and (b) P-TFTs input stage about slew rate and output swing.

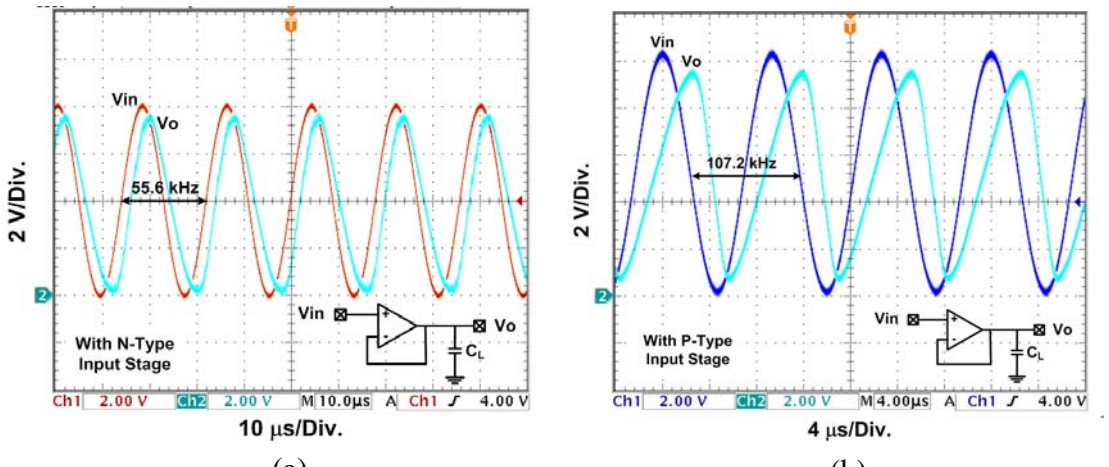

Fig. 4.15 The measured output waveforms of the class-A output buffers with (a) N-TFTs input stage and (b) P-TFTs input stage about unity-gain bandwidth.

The measured results of slew rate and output swing among 13 class-A output buffers with N-TFTs input stage are shown in Fig. 4.16. The output buffer with N-TFTs input stage really has poor manufacturing yield and performance stability due to the wider device variation. Based on the measured results in Fig. 4.14 and Fig. 4.15, obviously, we can find that the proposed output buffer with P-TFTs input stage has higher manufacturing yield and performance stability than those of the output buffer with N-TFTs input stage. The experimental results also have proven that replacing the critical part of the analog circuit by P-TFTs is a valid technique for suppressing device characteristic variation on glass substrate.

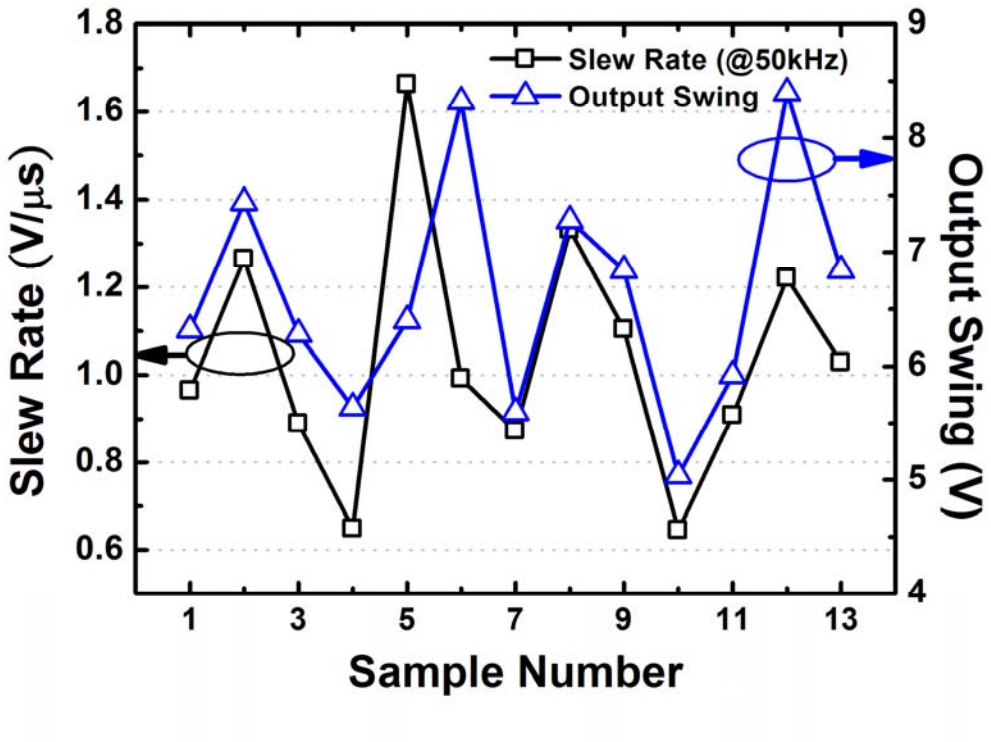

Fig. 4.16 The slew rate and output swing of the class-A output buffer with N-TFTs input stage, which are measured from 13 samples on glass substrate.

4.5 DISCUSSION

The accuracy of the data driver is determined by DAC circuit combined with analog output buffer. Even though the DAC has high accuracy, the data driver also has not enough accuracy with a low accuracy analog output buffer. For this reason, the input offset voltage of the analog output buffer will become a serious issue in data drivers. Fig. 4.17 shows a valid input offset compensation method and the measurement results of this analog output buffer with the offset compensation technique [22]. During the period I, the offset voltage is stored in C_H. In the period II, the detected offset voltage in C_H is added into the inverting input node. From Fig. 4.17 (b), we can find that the offset voltage of this analog output buffer can be compensated under the second period by using this offset compensation technique.

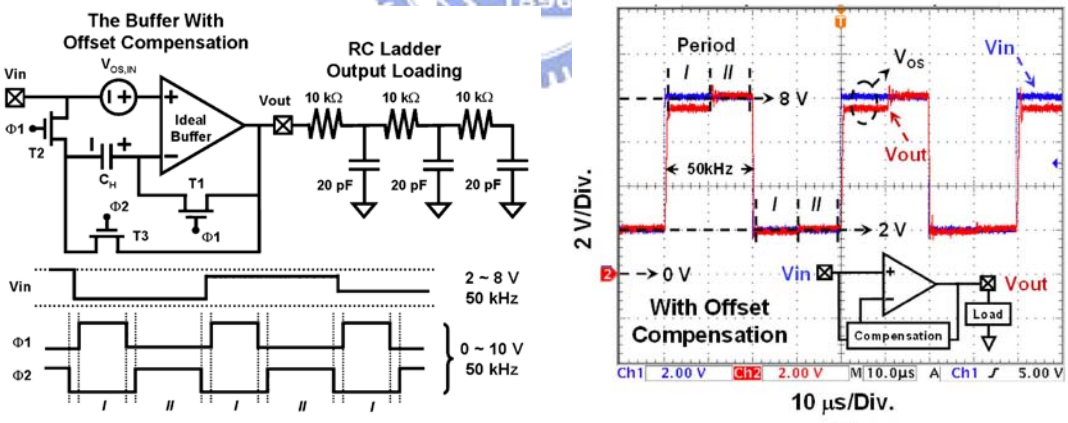

(a) (b)

Fig. 4.17 (a) Circuit and signal-timing diagram of the analog output buffer with the offset compensation technique. (b) The measurement result of this analog output buffer with the offset compensation technique under 50-kHz square wave with a swing of 2-to-8 V.

4.6 SUMMARY

In this chapter, A class-A output buffer with device variation suppressing technique in LTPS technology has been proposed and verified in 8-μm LTPS technology. The output buffer with P-TFTs input stage can be operated at 50-kHz operation frequency with at least 1-to-9 V output swing under V_{DD} of 10 V and V_{SS} of 0 V. The slew rate of this proposed output buffer is 1.961 V/μs. The device characteristic variation has been successfully suppressed by replacing the critical part of analog circuits by the P-TFTs. The proposed output buffer with P-TFTs input stage can be used in the on-panel data drivers to provide a uniform brightness and high resolution display. Furthermore, this proposed analog output buffer is also suitable for ambient light sensor system to boosting the output signal. Fig. 4.18 shows the proposed analog output buffers are used for pixel array in TFT-LCD panel.

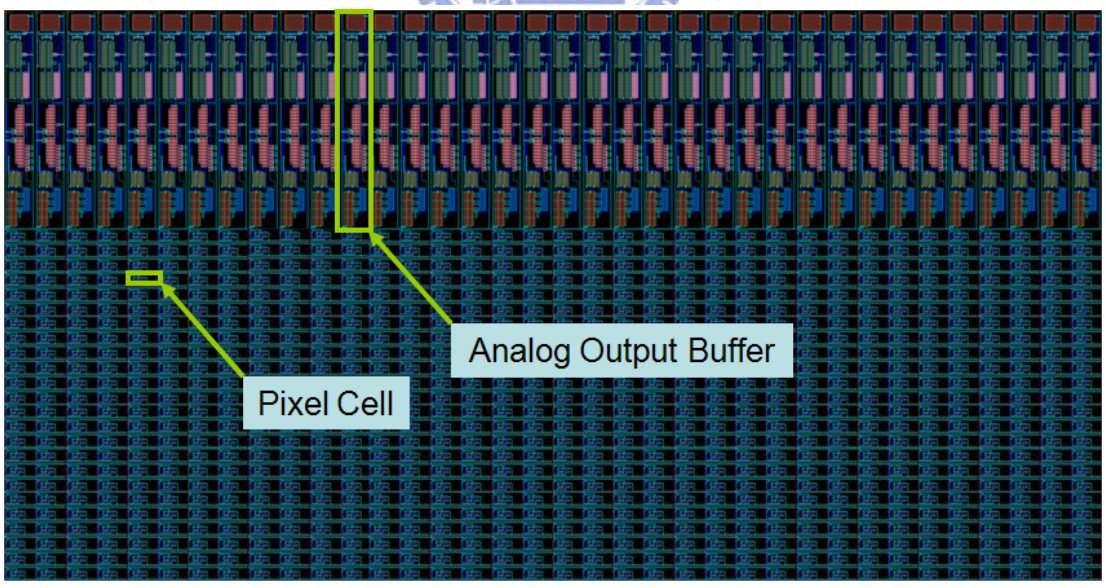

Fig. 4.18 The proposed class-A output buffer with P-TFTs input stage using for pixel array in TFT-LCD panel.